Journal of Volcanology and Geothermal Research 264 (2013) 223–230

Contents lists available at ScienceDirect

Journal of Volcanology and Geothermal Research

journal homepage: www.elsevier.com/locate/jvolgeores

The influence of wind on the estimation of lava effusion rate from thermal remote-sensing

F. Garel [a,b,c,*], E. Kaminski [a], S. Tait [a], A. Limare [a]

[a] Institut de Physique du Globe de Paris, Sorbonne Paris Cité, Univ. Paris Diderot, UMR CNRS 7154, 1 rue Jussieu, 75005 Paris, France
[b] Department of Earth Science and Engineering, Imperial College London, London SW7 2AZ, United Kingdom
[c] School of Earth and Ocean Sciences, Cardiff University, Cardiff CF10 3YE, United Kingdom

ARTICLE INFO

Article history:
Received 4 April 2013
Accepted 9 August 2013
Available online 28 August 2013

Keywords:
Volcanic hazard
Effusion rate
Thermal remote-sensing
Wind
Self-induced convection

ABSTRACT

Effusion rate is a key parameter to model lava flow advance and associated risks. Estimation of effusion rate from thermal remote-sensing using satellite data has matured to the point where it can be an operational monitoring tool, notably for volcanoes without a ground observatory. However, robust physical models, as required for quantitative interpretations, have not yet been adequately developed. The current and widely used method relates the satellite-measured radiated power to the flow effusion rate through the lava area, with an empirical fit that assumes a low surface cooling efficiency. Here we use novel fluid dynamic laboratory experiments and viscous flow theory to show that assuming low convective cooling at the surface of the flow leads to a systematic underestimation of the effusion rate. This result, obtained for the case of a hot isoviscous gravity current which cools as it flows, relies only on the respective efficiency of convection and radiation at the flow surface, and is independent of the details of the internal flow model. Applying this model to lava flows cooling under classical wind conditions, we find that the model compares well to data acquired on basaltic eruptions within the error bars corresponding to the uncertainties on natural wind conditions. Hence the thermal proxy deduced from the isoviscous model does not seem to require an additional fitting parameter accounting for internal flow processes such as crystallization. The predictions of the model are not correct however for thick lava flows such as highly viscous domes, because a thermal steady state is probably not reached for these flows. Furthermore, in the case of very large basaltic flows, extra cooling is expected due to self-induced convection currents. The increased efficiency of surface cooling for these large eruptions must be taken into account to avoid a gross – and dangerously misleading – underestimate of the effusion rate.

1. Introduction

A knowledge of magma discharge rate (effusion rate) is crucial for risk assessment on the flanks of a volcano (e.g. Guest et al., 1987; Ishihara et al., 1990; Vicari et al., 2009; Hérault et al., 2011), and is required to model, hence to anticipate, the advance of a lava flow during an effusive volcanic eruption (Walker, 1973; Griffiths, 2000). Effusion rate influences the regime of lava flow and cooling, with high effusion rates more likely to produce long, hazardous lava flow (Guest et al., 1987; Harris and Rowland, 2009). Retrieving the range and variation of effusion rate also brings information about the internal plumbing system of the volcano (Wadge, 1981). Gaining access to these key features requires the measurement or estimation of the effusion rate, as near as possible to real-time.

Effusion rate remains however an elusive parameter, hardly measurable in near real-time, and for which several proxies have been developed (see review in Harris et al. (2007)). Technologically advanced measurements using repeated plane-flown topographic surveys have been on occasion performed during a few eruptions on Mt. Etna (Coltelli et al., 2007; Favalli et al., 2010), but this remains costly and impractical as a general approach. One of the approaches currently most used to provide systematic quantitative measurements of effusion rate is thermal remote-sensing, exploiting satellite payloads. Since early pioneering studies (e.g. Glaze et al., 1989; Oppenheimer, 1991), this approach has steadily developed into a tool that has been used on several volcanoes (e.g. Harris et al., 2007; Spampinato et al., 2011). With respect to the more specific problem of real-time operational monitoring, a promising development has come with operation over the last few years of the SEVIRI payload on-board Meteosat (MSG2), which makes thermal radiance measurements every 15 min (Hirn et al., 2009; Ganci et al., 2012). For example, the *GMES-Downstream* project EVOSS makes operational use of SEVIRI to achieve continent-scale monitoring for countries with weak ground infrastructure that are nevertheless subject to serious volcanic risk (Ferrucci et al., 2013).

While thermal remote-sensing proxies are used as operational monitoring tools, there is still a need to better identify their limitations. Part of

* Corresponding author at: School of Earth and Ocean Sciences, Cardiff University, Cardiff CF10 3YE, United Kingdom. Tel.: +44 20 7594 7326.
E-mail address: GarelF@cardiff.ac.uk (F. Garel).

0377-0273/$ – see front matter © 2013 Elsevier B.V. All rights reserved.
http://dx.doi.org/10.1016/j.jvolgeores.2013.08.006

the uncertainty is related to the satellite measurement itself (e.g. Wright and Flynn, 2003; Ball and Pinkerton, 2006; Gouhier et al., 2012), and another part to the modeling and parameterization of the relationship between the thermal energy radiated at the surface of the flow and the flow rate (Dragoni and Tallarico, 2009; Harris and Baloga, 2009). In a previous study we have established a theoretical model relating the thermal structure of a hot isoviscous gravity current to its flow rate (Garel et al., 2012). This model gives one description of how the thermal evolution of the flow is controlled by the balance between heat advection within the flow, and heat lost at the surface by convection and radiation.

There are thus two major ways for improvement of the use of thermal-remote sensing techniques on lava flows: (1) more realistic modeling of heat advection within the flow (e.g. Filippucci et al. (2013)), with the possibility to take into account substrate geometries and complex rheologies with solidification, and (2) more precise description of effective heat loss at the surface of the flow by both radiation and convection in the air. The aim of the present paper is to quantify and discuss the effect of wind on lava flow cooling and on the resulting link between surface thermal signal and effusion rate.

2. Current thermal proxy

The thermal proxy in predominant current use is the time-independent model of Harris et al. (2007). Initially derived from a static heat budget for a lava flow that has stopped advancing (Pieri and Baloga, 1986), it was later applied to advancing lavas assuming that the heat losses at the surface and at the base of the lava flow are at all time balanced by the heat supplied by advection and crystallization (Harris et al., 1997), i.e. a kind of "frozen-time" approximation. This approximation is at odds with evidence for heat storage in the lava flow at the beginning of an eruption (Wooster et al., 1997). Nevertheless, Garel et al. (2012) have demonstrated that in the simple case of the spreading of a hot isoviscous, non-crystallizing fluid, initial heat storage in the current did not prevent the establishment of a thermal steady state after a transient period (during which the radiated power increased even though the input rate was constant). Hence this study established a first theoretical basis for the empirical relationship assuming proportionality between lava area and time-averaged effusion rate, which remains widely used (e.g. Wright et al., 2001; Harris et al., 2007; Harris and Baloga, 2009; Coppola et al., 2013).

The thermal proxy of Harris et al. (2007, 2010) is:

$$Q = \frac{\varepsilon\sigma\left(T_{top}^4 - T_a^4\right) + \lambda\left(T_{top} - T_a\right)}{c} A \quad (1)$$

with Q the effusion rate, A the lava flow area, ε the lava emissivity, σ the Stefan–Boltzmann constant, T_{top} the surface temperature of the lava flow, T_a the ambient temperature, λ the convective heat transfer coefficient (CHTC) that quantifies the convective cooling at the surface of the flow, and c a best-fit parameter, which should depend on the internal structure of the flow, on crystallization, on rheology and/or topography. The lava area A is derived from the satellite-measured power radiated by the flow assuming a range of possible surface temperatures (e.g. Wright et al. (2001)). The parameter c is defined by Harris et al. (1997) as $\rho(C_p\Delta T + \phi c_L)$, with ρ, ϕ, C_p, and c_L the lava density, crystal content, specific heat and latent heat of crystallization, respectively, and ΔT a temperature range (Harris et al., 2007, 2010). Note that Eq. (1) does not contain any reference to the flow dynamics (viscosity does not appear, for example). The detailed calculation of c remains controversial, as well as the physical justification of ΔT (Dragoni and Tallarico, 2009; Harris and Baloga, 2009). Recently, Coppola et al. (2013) introduced the global parameter of "radiant density" that integrates the influence of all control parameters into a unique best-fit coefficient given by the proportionality between lava area and effusion rate.

The maximal uncertainty on the calculation of the effusion rate from Eq. (1) is estimated around 50% (Harris et al., 2007). While significant, such an error is similar to the error on the estimate on average mass flux that might be achieved from ground-based measurements (Harris et al., 2007). The question remains however open about how the parameterization of surface cooling due to wind can introduce additional errors or can change the best-fit calculation in the estimation of effusion rate through Eq. (1). This issue is crucial for estimating uncertainties in the effusion rate calculation for poorly monitored volcanoes, considering that the best-fit relationship is established a posteriori (i.e. after the eruption).

We focus in the following on the influence of wind on the lava flows' thermal signature. All else being equal (effusion rate, topography, rheology) the influence of convective cooling depends only on the surface temperature of the flow and on the wind velocity, hence is independent of the treatment of the internal flow dynamics. We thus build on the theoretical and experimental model of Garel et al. (2012) to investigate quantitatively the influence of cooling by forced convection (wind).

3. Parameterization of convective cooling in the current thermal proxy

The rate of cooling of a lava flow with a surface temperature T_{top} occurs by radiation, which scales as $\varepsilon\sigma(T_{top}^4 - T_a^4)$, and by convection, either natural or forced by ambient winds, which scales as $\lambda(T_{top} - T_a)$. Radiation is the dominant heat transfer process when surface temperature T_{top} is still high. There is however a threshold surface temperature below which convection becomes the dominant heat loss process as the lava cools down (Head and Wilson, 1986; Keszthelyi et al., 2003). The surface temperature at which the two mechanisms switch roles as the dominant cooling process is higher for larger values of λ: 140, 300, 740 and 1010 °C for CHTC of 10, 20, 80 and 150 W m^{-2} K^{-1}, respectively, with an ambient temperature of 20 °C and an emissivity of 0.97.

In the absence of wind, natural convection (also called free convection) above the flow is driven by the buoyancy of the air heated by contact with the hot surface. For lava flows, the free CHTC λ has been theoretically estimated around 8–11 W m^{-2} K^{-1} (Keszthelyi and Denlinger, 1996; Neri, 1998). Most of the applications of the thermal proxy of Harris et al. (2007) use an average value of 10 W m^{-2} K^{-1}, i.e. implicitly assume only free convective cooling. However, wind (forced convection) is expected to increase the cooling rate at the surface of a lava flow (Neri, 1998).

This can be explained by a wind-induced thinning of the thermal boundary layer above the hot lava surface, which corresponds to larger CHTC λ, and which shows that contribution of ambient wind to convective cooling cannot be neglected a priori.

While the neglect of forced convection is likely to introduce a systematic bias on the estimation of eruption rates from the surface thermal signal of a lava flow, the rapid variations of wind in natural conditions (Keszthelyi et al., 2003) and the uncertainty on near real-time lava flow rate determination (Harris et al., 2007) make it difficult to provide a robust measurement of the convective cooling induced by ambient wind, hence of its quantitative consequences for the use of the thermal proxy. We thus perform laboratory experiments in controlled conditions to estimate the effect of forced convection on the surface thermal signal of a hot, viscous gravity current.

4. Experimental and theoretical investigation of wind-induced cooling

We measured the cooling of silicone oil, initially at a temperature T_0, spreading horizontally beneath air (at temperature $T_a < T_0$) onto a polystyrene plate, that is injected at a constant supply rate Q from a point source. A series of experiments with only natural convection in the air (i.e. no wind) was first performed with the set-up, and used to establish and validate a theoretical model for the cooling of an isoviscous gravity current (Garel et al., 2012). For the experiments used in this paper, we have added an additional experimental device blowing wind over the

silicone oil (see Appendix A). We performed experiments under two different wind conditions: one with an average velocity of 2.5 m s^{-1} (experiment C15) and the other with a velocity of 1.5 m s^{-1} (experiment C17). In order to assess the impact of the wind-induced cooling with respect to a reference case, the wind was systematically shut down at the end of the experiment, allowing a "wind-free" steady-state to be established, and hence the comparison to be made of the surface thermal structures of the current subject to natural rather than forced convection.

In the absence of wind the surface thermal signal becomes stationary in all experiments after a transient time corresponding to that required for the diffusion of heat to produce a stationary vertical profile of temperature in the current (Garel et al., 2012). Fig. 1 shows that the surface thermal structure of the current under forced convection also reaches a steady state after a transient time. A stationary hot tail anomaly develops downwind, due to the advection of air over the hot silicone oil. When the wind is shut down at the end of the experiment (i.e. the conditions go back to free convection), the surface thermal anomaly grows in size and in intensity, the hot tail disappears and the thermal structure becomes axisymmetric (see dynamic evolution in Supplementary Video). The radiated power ϕ_{rad} is defined as

$$\phi_{rad} = 2\pi \int_0^{R(t)} r\varepsilon\sigma\left(T_{top}^4(r,t) - T_a^4\right)\mathrm{d}r \tag{2}$$

$$= \iint_{\text{Flow area}} \varepsilon\sigma\left(T_{top}^4 - T_a^4\right)\mathrm{d}A, \tag{3}$$

with R the current radial extent at time t, r the radial coordinate, A the flow area, and with the same notation as in Eq. (1). The steady radiated power under free convection is always higher than under forced convection (Fig. 2). The net effect of forced convection, i.e. wind, is thus to reduce the radiated power for a given input rate. The reduction is about 70% for experiment C15 (2.5 m s^{-1} wind) and 60% for experiment C17 (1.5 m s^{-1} wind).

We model theoretically the cooling and spreading of the hot fluid by using the formalism of (Huppert, 1982) and the thermal model of Garel et al. (2012), see Appendix B for details. The key physical process related to the thermal proxy in this modeling is the heat lost at the surface of the flow by radiation and convection, the vertical surface heat flux (or heat flux density F_{tot}, in W m^{-2}) being locally

$$F_{tot} = \varepsilon\sigma\left(T_{top}^4 - T_a^4\right) + \lambda\left(T_{top} - T_a\right) \tag{4}$$

with the same notation as in Eq. (1). The total power is the integral of F_{tot} over the flow area, and is the sum of convective and radiative powers. In the following, we focus mainly on the radiated power ϕ_{rad}, because satellite sensors measure radiance data and not the total heat lost from the flow surface.

Fig. 3 shows the comparison between the wind-perpendicular surface temperature profile at steady state in experiment C15, and the prediction of the theoretical model of Garel et al. (2012). The comparison is made both for windy and non-windy conditions, taking in the theoretical model a λ equal to either 15 (2.5 m s^{-1} wind) or 2 W m^{-2} K^{-1} (free convection). The observed temperature profiles are different whether wind is blown across the current or not. The theoretical predictions are able to reproduce well the experimental data in both conditions (the inset of Fig. 3 shows the comparison for experiment C17, with a 1.5 m s^{-1} wind and $\lambda = 10$ W m^{-2} K^{-1}). The surface cooling of the experimental flow appears to depend largely on the value of λ which increases as a function of wind speed, and a constant "no-wind" value cannot reproduce the surface temperatures observed in windy conditions.

These results also confirm the expectation that the value of λ, hence the rate of cooling for a given mass flow rate, increases with wind velocity. This conclusion is in agreement with CHTC estimated for solar panels that have a horizontal length scale and surface temperature similar to our experiments, and that are exposed to natural wind (Sartori, 2006).

5. Implications for the thermal proxy of lava effusion rate

5.1. Wind conditions above lava flows

Wind measurements on lava flows which would allow the application of our approach to effusive eruptions remain scarce. Velocities between 2 and 12 m s^{-1} have been measured by Keszthelyi and Denlinger (1996), Harris et al. (1998), and Keszthelyi et al. (2003), and only two field estimates of the CHTC are available: $\lambda = 75$ W m^{-2} K^{-1} for a wind speed of 3 m s^{-1} (Keszthelyi and Denlinger, 1996), and $\lambda = 50$ W m^{-2} K^{-1} for a wind speed of 10 m s^{-1} (Keszthelyi et al., 2003). In a theoretical study, Neri (1998) proposed a CHTC about 60 W m^{-2} K^{-1} for a wind speed of 5 m s^{-1}. The discrepancy between these three estimates is due to the intrinsic difficulty of measuring λ, and to the many parameters that may affect its value (Head and Wilson, 1986; Neri, 1998; Patrick et al., 2004). They yield however the same order of magnitude of λ for the same order of magnitude of wind speed. All things being equal, they can be used to estimate the variation of λ with the wind speed using formula (9) of the theoretical study of Neri (1998) that we will express here as

$$\lambda = C_w V \tag{5}$$

where λ is the CHTC for a wind speed of V, and $C_w = 10$ J m^{-3} K^{-1} is a coefficient chosen such that $\lambda\,(V = 5\text{ m s}^{-1}) = 50$ W m^{-2} K^{-1}. For a wind speed ranging between 5 and 20 m s^{-1} (gale), the formula of Eq. (5) predicts a value of λ between 50 and 200 W m^{-2} K^{-1}. Acknowledging the variation in physical properties of the air at high temperatures (Neri, 1998; Patrick et al., 2004), we settle for a maximum range of possible λ over lava flows between 10 (free convection) and 150 W m^{-2} K^{-1}.

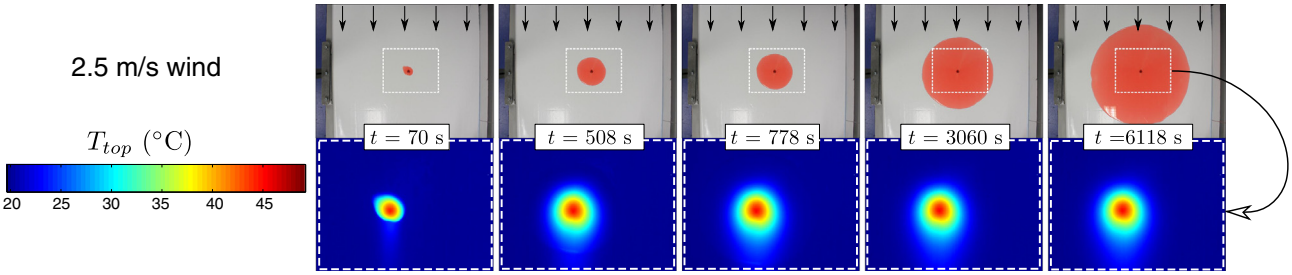

Fig. 1. Optical and infrared images taken during experiment C15 with wind blowing over the surface of the silicone oil, dyed red. The thermal infrared images give the surface temperature T_{top}. The white dashed rectangle in the optical picture matches the field of view of the infrared picture below. The black arrows give the direction of the 2.5 m s^{-1} wind. The hot tail downwind is observed because the silicone oil would otherwise be at ambient temperature, but is not expected in nature because lava, even solidified, remains hotter than the ambient air.

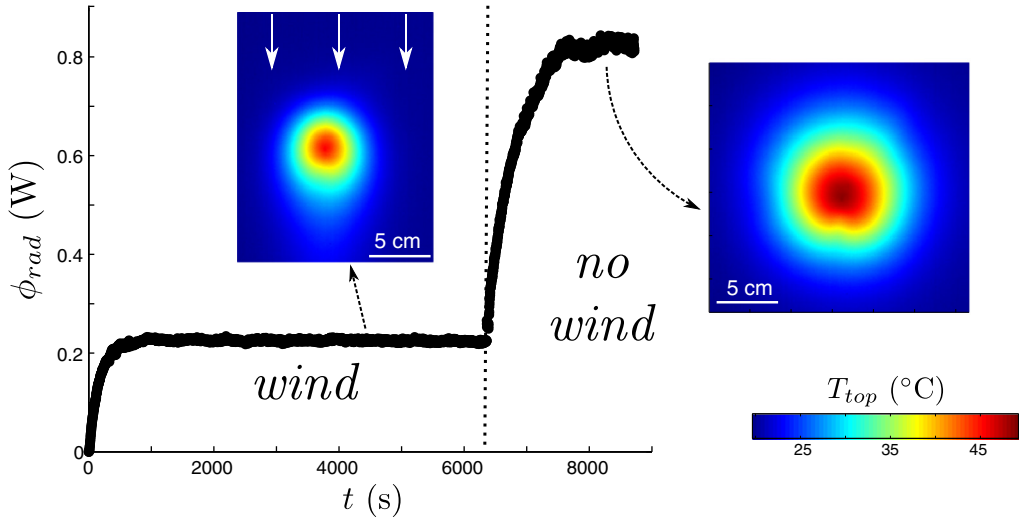

Fig. 2. Evolution of radiated power ϕ_{rad} as a function of time t for experiment C15. The liquid supply rate Q is constant throughout the experiment, but the wind has been shut down at 6360 s. The radiated power is computed for a radial surface temperature profile $T_{top}(r,t)$ normal to the wind direction. The steady surface thermal structures with or without wind are shown as infrared images. The dynamic evolution is shown in the Supplementary Video.

5.2. From radiated power to effusion rate

The theoretical model of Garel et al. (2012), detailed in Appendix B, provides first-order estimates of the total power radiated by a lava flow for a given effusion rate, once a thermal steady state has been achieved. Fig. 4 presents the comparison between the predictions of the model for basaltic lava flows and the field-data of effusion rate and radiated powers collected by Coppola et al. (2013) for different types of eruptions, and for three values of the CHTC: $\lambda = 10$ (free convection), $\lambda = 20$ (wind speed around 2 m s^{-1}), and $\lambda = 80$ W m^{-2} K^{-1} (wind speed around 8 m s^{-1}). There is a very good first-order agreement over several orders of magnitude between the observed and predicted relationship between radiated power and effusion rate for basaltic lavas. Furthermore, the variability of radiated power for a given effusion rate during the same eruption may be explained by a small variation in wind speed conditions between 2 and 8 m s^{-1}.

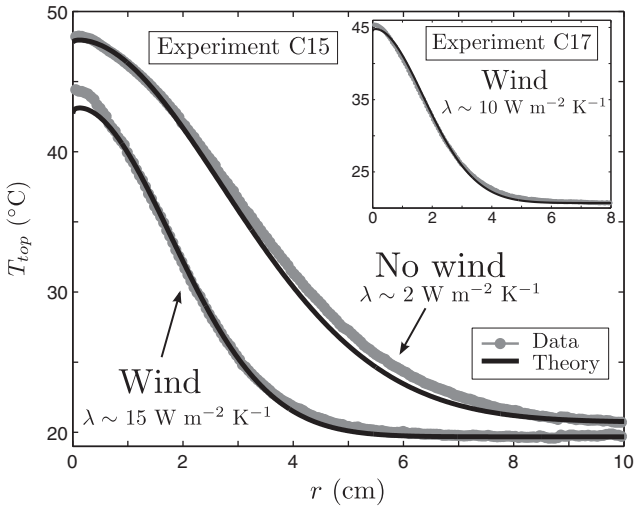

Fig. 3. Comparison of measured and predicted surface temperature profiles at steady state during experiment C15, under free or forced convection. The experimental surface temperatures T_{top} are given for a profile normal to the wind direction, with r the distance from the source. The inset gives the experimental measurements and theoretical prediction for a 1.5 m s^{-1} wind during experiment C17.

The reduction in radiated power (compared to the case of free convection with $\lambda = 10$ W m^{-2} K^{-1}) is around 35–40% for a λ of 20, and around 85% for a λ of 80 W m^{-2} K^{-1}. This reduction, that does not depend much on effusion rate, is smaller than in the experimental case since surface temperature are higher in the case of lava flows, hence radiative cooling is more important. Wind therefore appears as an extra-cause of radiance variations, in addition to previously identified controls of topography, rheology and crystallization (Harris et al., 2010; Coppola et al., 2013).

These results show that a simple isoviscous model of a hot gravity current is able to reproduce the field observations summarized in Coppola et al. (2013). On the other hand, there is a great discrepancy between the thermal signal of basaltic and acid lavas for the same effusion rate, which can be explained by the long transient stage expected for

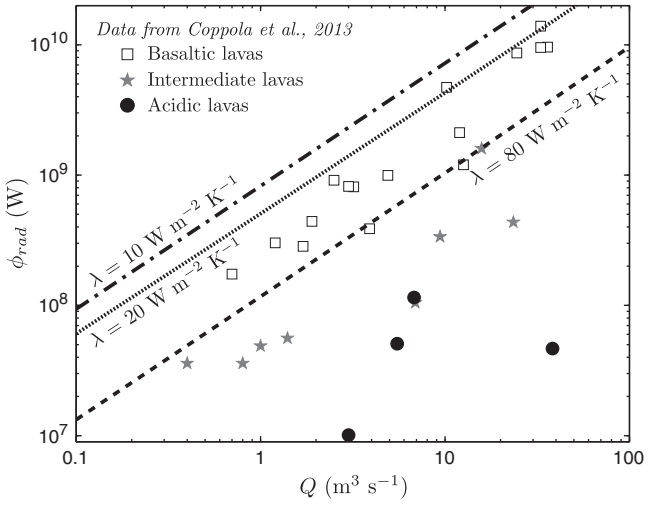

Fig. 4. Comparison between predicted and measured powers radiated by lava flows ϕ_{rad} as a function of their effusion rate Q. The data are from Coppola et al. (2013), with basaltic and intermediate lavas having SiO_2 content lower or equal to 50% or 60%, respectively, and acidic lava with more than 60% SiO_2. The theoretical predictions using the model of Garel et al. (2012) are the steady radiated powers with λ of 10 (dash-dotted line), 20 (thin dotted line) or 80 W m^{-2} K^{-1} (dashed line), and for the following parameters: emissivity $\varepsilon = 0.97$, source temperature $T_0 = 1100$ °C, ambient temperature $T_a = 20$ °C, viscosity $\mu = 1000$ Pa s, density $\rho = 2300$ kg m^{-3}, specific heat $C_p = 1000$ J kg^{-1} K^{-1} and thermal conductivity $k = 3$ W K^{-1} m^{-1}.

very viscous lavas (diffusive time of a few years!) before they exhibit a steady thermal signal (Garel et al., 2012).

Although Fig. 4 shows that the data of Coppola et al. (2013) are well flanked by the theoretical predictions for λ of 20 and 80 W m^{-2} K^{-1}, this result is somewhat at odds with the predictions of the (Harris et al., 2007) proxy that yields a good fit to the data with a fixed value of λ = 10 W m^{-2} K^{-1} (Harris et al., 2007). This suggests that a small best-fit parameter *c* of Eq. (1) compensates for the low value of λ. The radiated power data of Fig. 4 are only an estimate of the mean thermal signal measured during the eruptions, whereas the instantaneous radiated power can vary temporally as shown in Fig. 2a of Coppola et al. (2013). The data in Fig. 4 do not therefore give a definite conclusion on how to parameterize λ for the surface cooling of lava flows. Nevertheless, we recommend use of the values 20 and 80 W m^{-2} K^{-1}, respectively as lower and upper bounds for the CHTC (i.e. as upper and lower bounds for the estimated effusion rate), whichever thermal proxy is used. Cautious interpretation of instantaneous radiated power retrieved from thermal remote-sensing is nevertheless always necessary since the radiated power may vary with time if the effusion rate does.

The theoretical predictions of Fig. 4 give a first insight into the potential impact of convective cooling on the assessment of lava flow rate from measured radiated power. In Fig. 5 we quantify more explicitly this effect: the effusion rate is calculated as a function of the assumed CHTC for different radiated powers computed from satellite data. For a radiated power of 5 GW, the predicted effusion rate ranges from about 5 to 100 m^3 s^{-1} as the assumed λ varies from 5 to 150 W m^{-2} K^{-1}, since a larger and larger proportion of the supplied heat is evacuated from the flow by convective cooling as λ increases. Assuming λ = 80 W m^{-2} K^{-1} in the model, instead of the usual low value of 10 W m^{-2} K^{-1} value, will result in an increase of the calculated effusion rate by a factor 7–8 for any given radiated power. Fig. 5 also shows that the higher the radiated power, the larger the influence of the assumed λ on the calculated effusion rate.

Eq. (1), derived from the model of Harris et al. (2007), does not allow disentanglement of the lava area *A* from the relationship between effusion rate *Q* and radiated power. However, we can calculate the impact of assuming λ_{free} = 10 W m^{-2} K^{-1} (free convection) for a case with actual forced convection (λ_{wind}). The underestimate of the calculated effusion rate Q_{free} compared with the actual effusion rate Q_{wind} depends on the assumed surface temperature T_{top}:

$$R_Q = \frac{Q_{wind}}{Q_{free}} = \frac{\varepsilon\sigma\left(T_{top}^4 - T_a^4\right) + \lambda_{wind}\left(T_{top} - T_a\right)}{\varepsilon\sigma\left(T_{top}^4 - T_a^4\right) + \lambda_{free}\left(T_{top} - T_a\right)}. \quad (6)$$

Eq. (6) yields an underestimation factor R_Q that decreases as surface temperature (and radiative transfer) increases, and as λ gets closer to λ_{free} (Fig. 6). For λ_{wind} = 80 W m^{-2} K^{-1}, the underestimation on the effusion rate is of a factor 3.4 or 1.7, for surface temperatures T_{top} of 300 and 800 °C, respectively. This underestimate is thus lower than the one obtained from our model, because here we are able to take into account the influence of convective cooling on surface temperatures.

5.3. The case of very large basaltic eruptions

The data of Coppola et al. (2013), as shown in Fig. 4, suggest that the radiated power for small eruptions relates at first order to the effusion rate, with a significant but not dramatic influence of the wind conditions corresponding to λ smaller than 80 W m^{-2} K^{-1}. We expect a more serious effect above very large basaltic lava flows, since self-induced winds can indeed be generated from large surface heat flux inhomogeneities (e.g. Briggs, 1988; Kaminski et al., 2011) and yield very strong convective currents.

For example, very violent winds, that uprooted trees, were reported in the vicinity of the 20-km^2 lava flow of Mt. Nyiragongo emplaced on October 10th, 1977 (Tazieff, 1977). A violent wind storm also occurred during the January 17th, 2002 eruption of the same volcano that threatened the 400,000-inhabitant city of Goma (DRC), with wind destroying houses and roofs (Komorowski et al., 2002–2003). The wind speeds during these two eruptions can be estimated as above approximately 20 m s^{-1} from the damage they caused and according to the Beaufort scale.

A theoretical scaling derived for urban areas predicts that the wind velocity induced by surface heating scales as the one third power of the total (radiative and convective) surface power (Briggs, 1988; Wang, 2009). The storm events (e.g. 25 m s^{-1} associated with the Nyiragongo flows would correspond to a total surface power about 100 times larger than in the case of Hawaiian pahoehoe lava flows over which mild winds

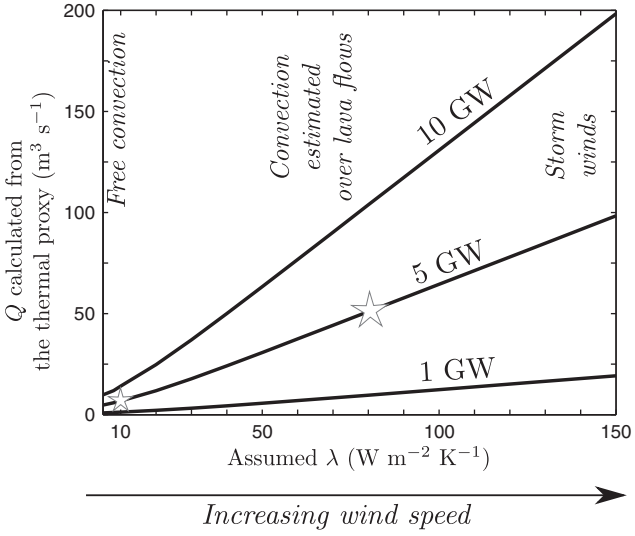

Fig. 5. Effusion rate Q calculated from the isoviscous model (Garel et al., 2012) assuming different CHTC λ, for a steady radiated power of 1, 5 or 10 GW. The stars give the effusion rates calculated for 5 GW and for a CHTC of 10 or 80 W m^{-2} K^{-1}. The parameters of the lava flow in the theoretical model are the same as in Fig. 4. The gray areas depict the expected values of λ for different external conditions.

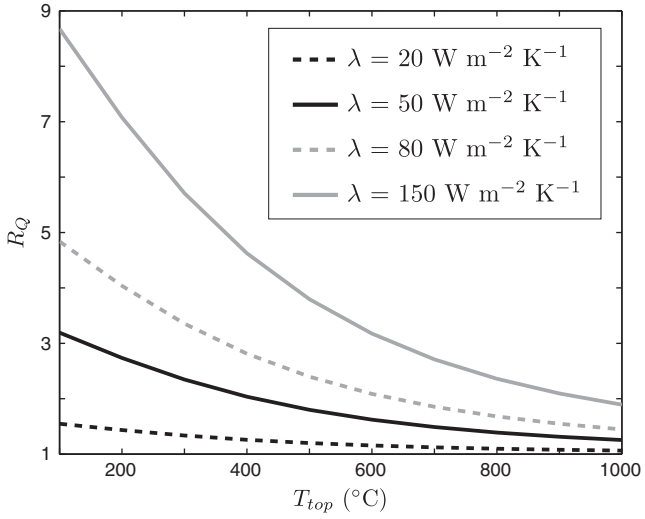

Fig. 6. Underestimation factor R_Q caused by assuming that the convective cooling occurs by free convection, as a function of the actual CHTC λ and of surface temperature T_{top} (Eq. (6)). The parameters (emissivity and ambient temperature) are the same as in Fig. 4. The conditions of large convective cooling (high λ and low surface temperature) yield the largest underestimate of the effusion rate.

(~5 m s^{-1}) were measured (Keszthelyi and Denlinger, 1996; Keszthelyi et al., 2003). This is consistent with the effusion rate estimated to be larger than 150 m^3 s^{-1} for the 1977 and 2002 Nyiragongo lava flows (Komorowski et al., 2002–2003), relative to about 2 m^3 s^{-1} for typical Hawaiian pahoehoe flows (Keszthelyi and Denlinger, 1996).

However the main issue in our opinion remains the quantification of the wind-induced convective cooling for storm conditions, and whether Eq. (5) or other engineering-based formula of forced convection (McAdams, 1954; Holman, 2010; Bejan, 2013), are still valid to draw a relationship between wind speed and CHTC. For example, Wells and Worster (2008) have shown that, for vertical surfaces, the laboratory-scale relationship to calculate the heat flux could not be extrapolated to the larger scales of geophysical applications. There seems to be at present no definite method to calculate an effective CHTC from the wind speed, the temperature, orientation and roughness of the surface, even though their respective influences are acknowledged (Neri, 1998; Chen, 2000; Freund et al., 2007; Palyvos, 2008; Turgut and Onur, 2010; Diani et al., 2013). This would be a valuable research area in order to better quantify the impact of wind strength on the surface convective cooling of lava flows, and also to investigate how the different surface thermal structures (e.g. cold solidified crust vs. hot melt exposed at the surface) influence wind circulation patterns over lava flows.

Because self-induced convection will induce a more efficient cooling of the lava flow, hence a lower surface temperature and a lower radiated power, all thermal proxies will tend to "saturate" when applied to huge effusion rates. For a flow rate of 200 m^3 s^{-1} for example, the radiated power under free convection predicted by the model of Garel et al. (2012) could reach up to 150 GW, whereas, when taking into account a maximal self-induced convection, we expect the radiated power to stall around 10 GW (Fig. 5), i.e. close to the maximum value observed for "regular" basaltic eruptions with no lava fountaining (Hirn et al., 2009). Hence we recommend that, for a radiated power larger than 10 GW, lower and upper bounds for the effusion rate are calculated taking a λ of 80 and of 150 W m^{-2} K^{-1} respectively, instead of the 20–80 W m^{-2} K^{-1} interval recommended for smaller basaltic eruptions.

6. Conclusion

The cooling induced by wind reduces the thermal power radiated by lava flows for a given effusion rate. Wind speeds measured over lava flows suggest that the currently used value of 10 W m^{-2} K^{-1} for λ is in reality a lower bound. A value of 80 W m^{-2} K^{-1}, on the other hand, provides an upper bound, which allows us to bracket the effusion rate. For small eruptions, the influence of convective cooling is within the uncertainty of field estimates of effusion rates, but there will be a systematic bias in the calculation of effusion rate from lava flow area if a value of $\lambda = 10$ W m^{-2} K^{-1} is used. For large eruptions with effusion rates greater than 100 m^3 s^{-1}, large-scale atmospheric convection is likely to develop, would result in a radiated power significantly lower than in the absence of wind. This would, by the same token, cause an underestimation of the effusion rate, if one uses the "regular" values for λ of 20–80 W m^{-2} K^{-1} instead of a more appropriate interval of 80–150 W m^{-2} K^{-1}. Meteorological monitoring could be a useful additional tool, as in the case of explosive volcanic eruptions (Le Pennec et al., 2012), to better estimate the wind strength over lava flows.

The theoretical model of Garel et al. (2012) predicts a bulk surface thermal signal for a spreading gravity current, whereas lava flows

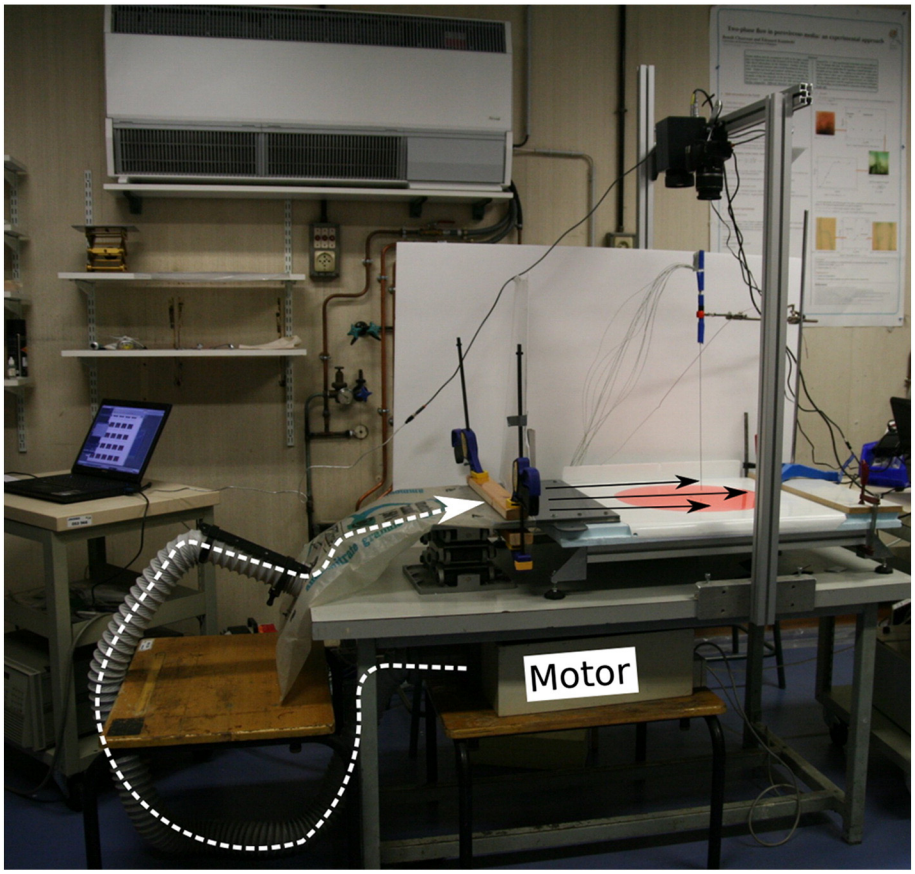

Fig. A.7. Photograph of the experimental set-up during experiment C17. The red silicone oil is spreading onto the polystyrene plate covered with teflon. The wind blower is a lab-made device: a sandblaster motor (under the table) blows air through a pipe into a plastic bag connected to thinly spaced horizontal plates resting on the polystyrene support. A drawer opened in the motor container enables the wind strength to be varied. The arrow indicates the path of the blown air.

exhibit a whole spectrum of surface temperatures (Flynn and Mouginis-Mark, 1994; Pinkerton et al., 2002). Although we cannot discuss here the use of satellite sensors at different wavelengths (sensitive to different ranges of surface temperatures), we point out that the decrease of radiated power due to forced convective cooling in the air will introduce a systematic bias in the evaluation of lava flow area from satellite data. Moreover, the signature of wind-enhanced cooling is likely to depend on the wavelengths considered in the satellite channels. It is therefore important for future studies to consider how windy conditions may affect the calculation of the radiated power from raw spectral radiances depending on each satellite sensor.

Further simultaneous field- and satellite-based data acquisition, including in-situ wind monitoring, would help to better constrain how our first-order scaling of the influence of wind on their surface thermal signal can be extrapolated to natural, large-scale lava flows.

Supplementary data to this article can be found online at http://dx.doi.org/10.1016/j.jvolgeores.2013.08.006.

Acknowledgments

We acknowledge Yves Gamblin for his help with the experimental device, and Damien Gaudin for the loan of the infrared camera. We thank Diego Coppola and one anonymous reviewer for useful comments on this manuscript, and are grateful to Lionel Wilson for the editorial handling.

Appendix A. Details of the experimental settings

The apparatus designed to study the surface thermal structure of silicone oil (Rhodorsil 47 V 5000, dyed red), injected at a constant rate and spreading horizontally from a point source is described in a previous paper (Garel et al., 2012).

An experimental device is added to blow a controlled wind over the spreading oil, in order to enhance convective cooling by forced convection (Fig. A.7).

The wind speed over the plate is measured with a Testo hot-wire anemometer (Fig. A.8). As expected, the wind speed decreases away from the blower and is maximum at the center of the plate. The average wind speed in a circle of radius 5 cm around the point source (about the size of the thermal anomaly) is about 2.5 m s^{-1} in the case of experiment C15, for which the drawer of the motor container is only opened 10 cm. When the drawer aperture is about 14 cm, the average wind speed is 1.5 m s^{-1} (experiment C17). The wind remains sufficiently low not to disturb the axisymmetric oil advance, since the viscous spreading is in agreement with the predictions based in the theory of viscous gravity current spreading (Huppert, 1982).

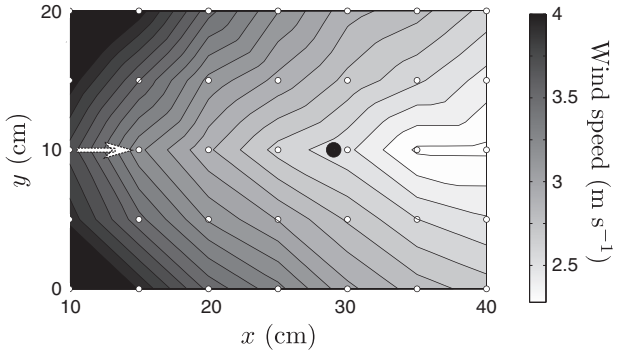

Fig. A.8. Map view of the wind speed on the experimental plate for a drawer aperture of 10 cm. The wind direction is indicated by the white arrow. The wind values are extrapolated from 5-cm spaced measurements (white circles). The black dot represents the injection point. The hot wire of the anemometer is less than a centimeter above the plate during the measurements.

Table A.1
Experimental parameters and conditions for the experiments with silicone oil and imposed wind.

Name	Duration	Q (m^3 s^{-1})	T_0 (°C)	T_a (°C)	μ_o[a] (pa s)	ρ_o[a] kg m^{-3}	Wind speed (m s^{-1})
C15	2 h 32 min	$2.6\,10^{-8}$	48	20	3.0	949	2.5
C17	2 h 54 min	$1.9\,10^{-8}$	49	20	3.0	948	1.5

[a] μ_o and ρ_o are the viscosity and density at source temperature T_0.

Table A.1 presents the conditions for the two experiments with silicone oil over which wind was blown. For the two experiments, the wind was shut down after some time in order to image the reference steady thermal signal unaffected by the wind.

Appendix B. Details of the theoretical model

As stated in the main text, the Navier–Stokes equations describing the advance of an isoviscous flow are the ones of Huppert (1982). The conservation of energy over the vertical domain, assuming isolating conditions at the flow base, writes (Garel et al., 2012)

$$\frac{\partial}{\partial t}\left(\int_0^{h(r,t)} T\mathrm{d}z\right) = -\frac{1}{r}\frac{\partial}{\partial r}\left(r\int_0^{h(r,t)} uT\mathrm{d}z\right) + \kappa\frac{\partial T}{\partial z}|_{z=h}, \tag{B.1}$$

where h, T, and u are the current thickness, temperature, and horizontal velocity, respectively, and κ is the thermal diffusivity of the fluid. The second term on the right handside of Eq. (B.1) is the vertical heat flux at the surface of the flow F_{tot} (Eq. (4)).

The non-dimensionalization of Eq. (B.1) yields three dimensionless numbers N_T, N_λ and N_{surf}:

$$N_T = \frac{T_0 - T_a}{T_0} \tag{B.2}$$

$$N_\lambda = \frac{\lambda}{\epsilon\sigma T_0^3 + \lambda} \tag{B.3}$$

$$N_{surf} = \frac{\epsilon\sigma T_0^4 + \lambda T_0}{k_{\frac{T_0}{h_{ref}}}}, \tag{B.4}$$

with k the thermal conductivity and h_{ref} the reference height of the current defined by Huppert (1982), and function of the flow viscosity and input rate. These dimensionless numbers characterize the amount of energy input at the source, the amount of convective vs. radiative heat cooling, and the global efficiency of surface cooling versus vertical thermal diffusion, respectively.

The power radiated by the current ϕ_{rad} is predicted to become steady after a transient time. The duration of the transient stage is the time required for the current to establish a steady radial thermal anomaly around the source, and the transient time shortens as the cooling efficiency increases. For lava flows, N_{surf} is very high and the transient time is close to the diffusive time h_{ref}^2/κ. The predicted values for steady area and radiated power as a function of the effusion rate Q for lava flow parameters are given in Garel et al. (2012).

References

Ball, M., Pinkerton, H., 2006. Factors affecting the accuracy of thermal imaging cameras in volcanology. J. Geophys. Res. 111, B11203.
Bejan, A., 2013. Convection Heat Transfer. John Wiley & Sons, New York.
Briggs, G., 1988. Surface inhomogeneity effects on convective diffusion. Bound.-Layer Meteorol. 45, 117–135.
Chen, C.H., 2000. Heat transfer characteristics of a non-isothermal surface moving parallel to a free stream. Acta Mech. 142, 195–205.
Coltelli, M., Proietti, C., Branca, S., Marsella, M., Andronico, D., Lodato, L., 2007. Analysis of the 2001 lava flow eruption of Mt. Etna from three-dimensional mapping. J. Geophys. Res. 112, F02029.

Coppola, D., Laiolo, M., Piscopo, D., Cigolini, C., 2013. Rheological control on the radiant density of active lava flows and domes. J. Volcanol. Geotherm. Res. 249, 39–48.
Diani, A., Mancin, S., Zilio, C., Rossetto, L., 2013. An assessment on air forced convection on extended surfaces: experimental results and numerical modeling. Int. J. Therm. Sci. 67, 120–134.
Dragoni, M., Tallarico, A., 2009. Assumptions in the evaluation of lava effusion rates from heat radiation. Geophys. Res. Lett. 36, L08302.
Favalli, M., Fornaciai, A., Mazzarini, F., Harris, A., Neri, M., Behncke, B., Pareschi, M., Tarquini, S., Boschi, E., 2010. Evolution of an active lava flow field using a multitemporal LIDAR acquisition. J. Geophys. Res. 115, B11203.
Ferrucci, F., Theys, N., Clarisse, L., Hirn, B., Laneve, G., Valks, P., Van der, A.R., Tait, S., Di Bartola, C., Brenot, H., 2013. Operational integration of spaceborne measurements of Lava discharge rates and Sulphur Dioxide concentrations for Global Volcano Monitoring. In: Wenzel, F., Zschau, J. (Eds.), Early Warning for Geological Disasters – Scientific Methods and Current Practice, Springer.
Filippucci, M., Tallarico, A., Dragoni, M., 2013. Role of heat advection in a channeled lava flow with power law, temperature-dependent rheology. J. Geophys. Res. Solid Earth 118 (6), 2764–2776 (June).
Flynn, L., Mouginis-Mark, P., 1994. Temperature of an active lava channel from spectral measurements, Kilauea Volcano, Hawaii. Bull. Volcanol. 56, 297–301.
Freund, S., Pautsch, A., Shedd, T., Kabelac, S., 2007. Local heat transfer coefficients in spray cooling systems measured with temperature oscillation IR thermography. Int. J. Heat Mass Transf. 50, 1953–1962.
Ganci, G., Harris, A., Del Negro, C., Guehenneux, Y., Cappello, A., Labazuy, P., Calvari, S., Gouhier, M., 2012. A year of lava fountaining at Etna: volumes from SEVIRI. Geophys. Res. Lett. 39, L06305.
Garel, F., Kaminski, E., Tait, S., Limare, A., 2012. An experimental study of the surface thermal signature of hot subaerial isoviscous gravity currents: implications for thermal monitoring of lava flows and domes. J. Geophys. Res. 117, B02205.
Glaze, L., Francis, P., Rothery, D., 1989. Measuring thermal budgets of active volcanoes by satellite remote sensing. Nature 338, 144–146.
Gouhier, M., Harris, A., Calvari, S., Labazuy, P., Guéhenneux, Y., Donnadieu, F., Valade, S., 2012. Lava discharge during Etna's January 2011 fire fountain tracked using MSG-SEVIRI. Bull. Volcanol. 74, 787–793.
Griffiths, R.W., 2000. The dynamics of lava flows. Annu. Rev. Fluid Mech. 32, 477–518.
Guest, J., Kilburn, C., Pinkerton, H., Duncan, A., 1987. The evolution of lava flow-fields: observations of the 1981 and 1983 eruptions of Mount Etna, Sicily. Bull. Volcanol. 49, 527–540.
Harris, A., Baloga, S., 2009. Lava discharge rates from satellite-measured heat flux. Geophys. Res. Lett. 36, L19302.
Harris, A., Rowland, S., 2009. Effusion rate controls on lava flow length and the role of heat loss: a review. In: Thordarson, T., Self, S., Larsen, G., Rowland, S.K., Hoskuldsson, A. (Eds.), Studies in Volcanology: The Legacy of George Walker. Special Publications of IAVCEI, pp. 33–51.
Harris, A., Blake, S., Rothery, D., Stevens, N., 1997. A chronology of the 1991 to 1993 Mount Etna eruption using advanced very high resolution radiometer data: implications for real-time thermal volcano monitoring. J. Geophys. Res. 102, 7985–8003.
Harris, A., Flynn, L., Keszthelyi, L., Mouginis-Mark, P., Rowland, S., Resing, J., 1998. Calculation of lava effusion rates from Landsat TM data. Bull. Volcanol. 60, 52–71.
Harris, A., Dehn, J., Calvari, S., 2007. Lava effusion rate definition and measurement: a review. Bull. Volcanol. 70, 1–22.
Harris, A., Favalli, M., Steffke, A., Fornaciai, A., Boschi, E., 2010. A relation between lava discharge rate, thermal insulation, and flow area set using lidar data. Geophys. Res. Lett. 37, L20308.
Head III, J., Wilson, L., 1986. Volcanic processes and landforms on Venus: theory, predictions, and observations. J. Geophys. Res. 91, 9407–9446.
Hérault, A., Bilotta, G., Vicari, A., Rustico, E., Del Negro, C., 2011. Numerical simulation of lava flow using a GPU SPH model. Ann. Geophys. 54.
Hirn, B., Di Bartola, C., Ferrucci, F., 2009. Combined use of SEVIRI and MODIS for detecting, measuring, and monitoring active lava flows at erupting volcanoes. IEEE Trans. Geosci. Remote Sens. 47, 2923–2930.
Holman, J., 2010. Heat Transfer, 10th edition. McGraw-Hill, London.
Huppert, H., 1982. Propagation of two-dimensional and axisymmetric viscous gravity currents over a rigid horizontal surface. J. Fluid Mech. 121, 43–58.
Ishihara, K., Iguchi, M., Kamo, K., 1990. Numerical simulation of lava flows on some volcanoes in Japan. Lava Flows and Domes: Emplacement Mechanisms and Hazard Implications. Springer-Verlag, pp. 174–207.
Kaminski, E., Chenet, A., Jaupart, C., Courtillot, V., 2011. Rise of volcanic plumes to the stratosphere aided by penetrative convection above large lava flows. Earth Planet. Sci. Lett. 301, 171–178.
Keszthelyi, L., Denlinger, R., 1996. The initial cooling of pahoehoe flow lobes. Bull. Volcanol. 58, 5–18.
Keszthelyi, L., Harris, A., Dehn, J., 2003. Observations of the effect of wind on the cooling of active lava flows. Geophys. Res. Lett. 30.
Komorowski, J., Tedesco, D., Kasereka, M., Allard, P., Papale, P., Vaselli, O., Durieux, J., Baxter, P., Halbwachs, M., Akumbe, M., et al., 2002–2003. The January 2002 flank eruption of Nyiragongo volcano (Democratic Republic of Congo): chronology, evidence for a tectonic trigger, and impact of lava flows on the city of Goma. Acta Vulcanol. 14–15, 27–61.
Le Pennec, J., Ruiz, G., Ramon, P., Palacios, E., Mothes, P., Yepes, H., 2012. Impact of Tephra falls on Andean communities: the influences of eruption size and weather conditions during the 1999–2001 activity of Tungurahua volcano, Ecuador. J. Volcanol. Geotherm. Res. 217–218, 91–103.
McAdams, W.H., 1954. Heat Transmission. McGraw-Hill, New York.
Neri, A., 1998. A local heat transfer analysis of lava cooling in the atmosphere: application to thermal diffusion-dominated lava flows. J. Volcanol. Geotherm. Res. 81, 215–243.
Oppenheimer, C., 1991. Lava flow cooling estimated from Landsat Thematic Mapper infrared data: the Lonquimay eruption (Chile, 1989). J. Geophys. Res. 96, 21865–21878.
Palyvos, J., 2008. A survey of wind convection coefficient correlations for building envelope energy systems modeling. Appl. Therm. Eng. 28, 801–808.
Patrick, M.R., Dehn, J., Dean, K., 2004. Numerical modeling of lava flow cooling applied to the 1997 Okmok eruption: approach and analysis. J. Geophys. Res. 109, B03202.
Pieri, D., Baloga, S., 1986. Eruption rate, area, and length relationships for some Hawaiian lava flows. J. Volcanol. Geotherm. Res. 30, 29–45.
Pinkerton, H., James, M., Jones, A., 2002. Surface temperature measurements of active lava flows on Kilauea volcano, Hawai'i. J. Volcanol. Geotherm. Res. 113, 159–176.
Sartori, E., 2006. Convection coefficient equations for forced air flow over flat surfaces. Sol. Energy 80, 1063–1071.
Spampinato, L., Calvari, S., Oppenheimer, C., Boschi, E., 2011. Volcano surveillance using infrared cameras. Earth Sci. Rev. 106, 63–91.
Tazieff, H., 1977. An exceptional eruption: Mt Nyiragongo, Jan. 10th, 1977. Bull. Volcanol. 40, 189–200.
Turgut, O., Onur, N., 2010. An experimental and three dimensional numerical study on the wind-related heat transfer from a rectangular flat plate model collector flush mounted on the roof of a model house. Heat Mass Transf. 46, 1345–1354.
Vicari, A., Ciraudo, A., Del Negro, C., Herault, A., Fortuna, L., 2009. Lava flow simulations using discharge rates from thermal infrared satellite imagery during the 2006 Etna eruption. Nat. Hazard. 50, 539–550.
Wadge, G., 1981. The variation of magma discharge during basaltic eruptions. J. Volcanol. Geotherm. Res. 11, 139–168.
Walker, G., 1973. Lengths of lava flows. Philos. Trans. R. Soc. Lond. A 274, 107–116.
Wang, W., 2009. The influence of thermally-induced mesoscale circulations on turbulence statistics over an idealized urban area under a zero background wind. Bound.-Layer Meteorol. 131, 403–423.
Wells, A.J., Worster, M.G., 2008. A geophysical-scale model of vertical natural convection boundary layers. J. Fluid Mech. 609, 111–138.
Wooster, M., Wright, R., Blake, S., Rothery, D., 1997. Cooling mechanisms and an approximate thermal budget for the 1991–1993 Mount Etna lava flow. Geophys. Res. Lett. 24, 3277–3280.
Wright, R., Flynn, L., 2003. On the retrieval of lava-flow surface temperatures from infrared satellite data. Geology 31, 893–896.
Wright, R., Blake, S., Harris, A., Rothery, D., 2001. A simple explanation for the space-based calculation of lava eruption rates. Earth Planet. Sci. Lett. 192, 223–233.